Acta Crystallographica Section F
Structural Biology Communications
ISSN 2053-230X

Crystallization and preliminary X-ray diffraction studies of an L-amino-acid oxidase from *Lachesis muta* venom

Anwar Ullah,[a] Rehana Masood,[a] Patrick Jack Spencer,[b] Mário Tyago Murakami[c] and Raghuvir Krishnaswamy Arni[a]*

[a]Department of Physics, UNESP/IBILCE, Rua Cristovão Colombo 2265, São José Do Rio Preto, São Paulo 15054-000, Brazil, [b]Comissão Nacional de Energia Nuclear, Instituto de Pesquisas Energéticas e Nucleares, IPEN, São Paulo 05508-900, Brazil, and [c]Laboratório Nacional de Biociências (LNBio), Centro Nacional de Pesquisa em Energia e Materiais, Campinas 13083-970, Brazil

Correspondence e-mail: arni@sjrp.unesp.br

Received 12 May 2014
Accepted 2 August 2014

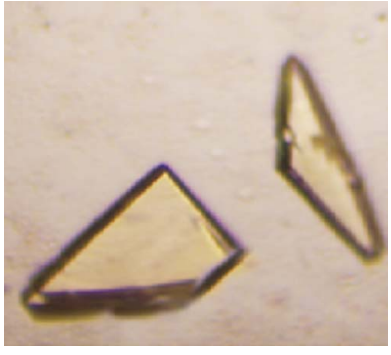

Snake-venom proteins form multi-component defence systems by the recruitment and rapid evolution of nonvenomous proteins and hence serve as model systems to understand the structural modifications that result in toxicity. L-Amino-acid oxidases (LAAOs) are encountered in a number of snake venoms and have been implicated in the inhibition of platelet aggregation, cytotoxicity, haemolysis, apoptosis and haemorrhage. An L-amino-acid oxidase from *Lachesis muta* venom has been purified and crystallized. The crystals belonged to space group $P2_1$, with unit-cell parameters $a = 66.05$, $b = 79.41$, $c = 100.52$ Å, $\beta = 96.55^\circ$. The asymmetric unit contained two molecules and the structure has been determined and partially refined at 3.0 Å resolution.

1. Introduction

Snake venoms, which are used for attack, defence and digestion, are complex mixtures of proteins, enzymes and biologically active peptides that interfere with key physiological processes, triggering a wide spectrum of secondary effects such as blood coagulation, myotoxicity, neurotoxicity, platelet aggregation and lipid digestion (Lewis & Garcia, 2003). Structural studies of these proteins are relevant since it has been suggested that mammalian proteins involved in key regulatory processes have been recruited, modified and expressed in the venom gland to function as toxins (Fry, 2005).

Lachesis muta envenomation causes extensive tissue damage, hypotension and shock, and can result in death owing to the neurotoxic, haemorrhagic and coagulant activities of the venom (Jorge *et al.*, 1997)

L-Amino-acid oxidases (LAAOs; EC 1.4.3.2) are homodimeric enzymes which, together with the noncovalently bound cofactor flavin adenine dinucleotide (FAD), catalyse the oxidative deamination of L-amino acids to the corresponding α-keto acids with the concomitant liberation of ammonia (NH_3) and hydrogen peroxide (H_2O_2) and the reduction of FAD (Zhang *et al.*, 2003; Sun *et al.*, 2010). In addition to snake-gland secretions, LAAOs are encountered in many other organisms such as fungi, bacteria, fish skin mucus and plants (Arima *et al.*, 2009; Yang *et al.*, 2009; Kitani *et al.*, 2007; Nagashima *et al.*, 2009; Du & Clemetson, 2002; Kasai *et al.*, 2010; Stábeli *et al.*, 2007), where they are involved in the utilization of nitrogen sources (Du & Clemetson, 2002). LAAOs from snake venoms are cytotoxic, apoptotic, inhibit platelet agreggation and display bactericidal and antiviral activities (Rodrigues *et al.*, 2009; Alves *et al.*, 2008; Li *et al.*, 1994; Stábeli *et al.*, 2007; Zhang *et al.*, 2003).

LAAOs are homodimeric glycosylated proteins with molecular weights ranging from 110 to 150 kDa (Stábeli *et al.*, 2007; Du & Clemetson, 2002). Each subunit is composed of three domains: a FAD-binding domain, a substrate-binding domain and a helical domain (Georgieva *et al.*, 2011; Zhang *et al.*, 2004; Faust *et al.*, 2007; Kang *et al.*, 2011; Ullah, Souza *et al.*, 2012).

The crystal structures of LAAOs from *Calloselasma rhodostoma* (PDB entry 1f8r; 2.0 Å resolution; Moustafa *et al.*, 2006), *Agkistrodon halys pallas* (PDB entry 1reo; 2.3 Å resolution; Zhang *et al.*, 2004), *Vipera ammodytes ammodytes* (PDB entry 3kve; 2.6 Å resolution; Georgieva *et al.*, 2011) and *Bothrops jararacussu* (PDB entry 4e0v; 3.1 Å resolution; Ullah *et al.*, 2012) have been determined. The crystal

Table 1
Crystallization.

Method	Hanging-drop vapour diffusion
Plate type	24-well tissue-culture plate
Temperature (K)	291
Protein concentration (mg ml^{-1})	11
Buffer composition of protein solution	0.02 *M* Tris–HCl pH 8.0
Composition of reservoir solution	0.2 *M* ammonium acetate, 20%(*w*/*v*) PEG 3350 pH 7.1
Volume and ratio of drop	1 µl protein solution + 1 µl reservoir solution
Volume of reservoir (ml)	0.5

structure of the LAAO from *C. rhodostoma* in the presence of bound substrate provides detailed information on the mechanism of action of this enzyme (Moustafa *et al.*, 2006). In the crystal structure of LAAO from *V. ammodytes ammodytes*, a Zn^{2+} ion stabilizes the quaternary structure of this enzyme and is considered important for its enzymatic activity (Georgieva *et al.*, 2011). In the crystal structure of LAAO from *B. jararacussu* the FAD was encountered in two different conformations and this enzyme shows a marked preference for hydrophobic amino acids (Ullah, Coronado *et al.*, 2012).

Here, we present the purification and crystallization of an LAAO from *L. muta* venom (LmLAAO). The structural analysis of this enzyme along with functional and structural investigation of other snake-venom LAAOs, which is being carried out by our group, will contribute towards understanding the correlation between toxicity and three-dimensional structure (Ullah, Coronado *et al.*, 2012; Ullah, Souza *et al.*, 2012; Georgieva *et al.*, 2011).

2. Materials and methods

2.1. Venom collection and purification

Desiccated crude *L. muta* venom was obtained from the Sanmaru Serpentarium (SANMARU Ltda, Taquaral, São Paulo, Brazil). 150 mg of the venom was dissolved in 2.5 ml 0.02 *M* Tris–HCl buffer pH 8.0 containing 0.1 *M* NaCl and was centrifuged at 10 000*g* for 10 min. The clear supernatant was divided into two fractions that were separately subjected to size-exclusion chromatography on a Sephacryl S-200 column previously equilibrated with the aforementioned buffer. The proteins were eluted at a flow rate of 0.2 ml min^{-1}, the absorbance was monitored at 280 nm and 1 ml fractions were collected.

The factions corresponding to peak 1a from the two runs of size-exclusion chromatography (results not shown) were pooled and applied onto a Mono S 5/50 GL column. The column was then washed with the loading buffer until the baseline returned to the initial value. The bound protein fractions were eluted with a nonlinear gradient of the same buffer containing 1 *M* NaCl. All fractions were concentrated and the purity was evaluated by SDS–PAGE (Laemmli, 1970).

2.2. Crystallization

The LmLAAO sample was dialyzed against 0.02 *M* Tris–HCl pH 8.0 and concentrated to 11 mg ml^{-1} in microconcentrators with a 30 kDa cutoff. Crystallization experiments were performed by the hanging-drop vapour-diffusion method in 24-well tissue-culture plates (Jancarik & Kim, 1991) using commercially available crystallization screens such as Crystal Screen, Crystal Screen 2, Grid Screen PEG 6000, Grid Screen Ammonium Sulfate, PEG/Ion (Hampton Research) and The PEGs Suite (Qiagen). Typically, 1 µl drops of protein solution were mixed with an equal volume of the screening solution and equilibrated over a reservoir containing 0.5 ml of the latter solution. Crystals suitable for X-ray diffraction experiments were obtained when the reservoir consisted of 0.2 *M* ammonium acetate, 20%(*w*/*v*) PEG 3350 pH 7.1. Crystallization is summarized in Table 1.

2.3. Data collection and processing

For X-ray diffraction data collection, an LmLAAO crystal was directly flash-cooled in a 100 K nitrogen-gas stream on the W01B-MX2 beamline of the Brazilian Synchrotron Light Laboratory (LNLS), Campinas, Brazil. The wavelength of the radiation source was set to 1.458 Å and a MAR Mosaic 225 mm CCD detector was used to record the X-ray diffraction intensities. The LAAO crystal was exposed for 90 s per degree of rotation around φ; a total of 181 images were collected and the crystal-to-detector distance was set to 100 mm. The data were indexed, integrated and scaled using the *DENZO* and *SCALEPACK* programs from the *HKL*-2000 package (Otwinowski & Minor, 1997). Data-collection and processing statistics are summarized in Table 2. Molecular replacement was carried

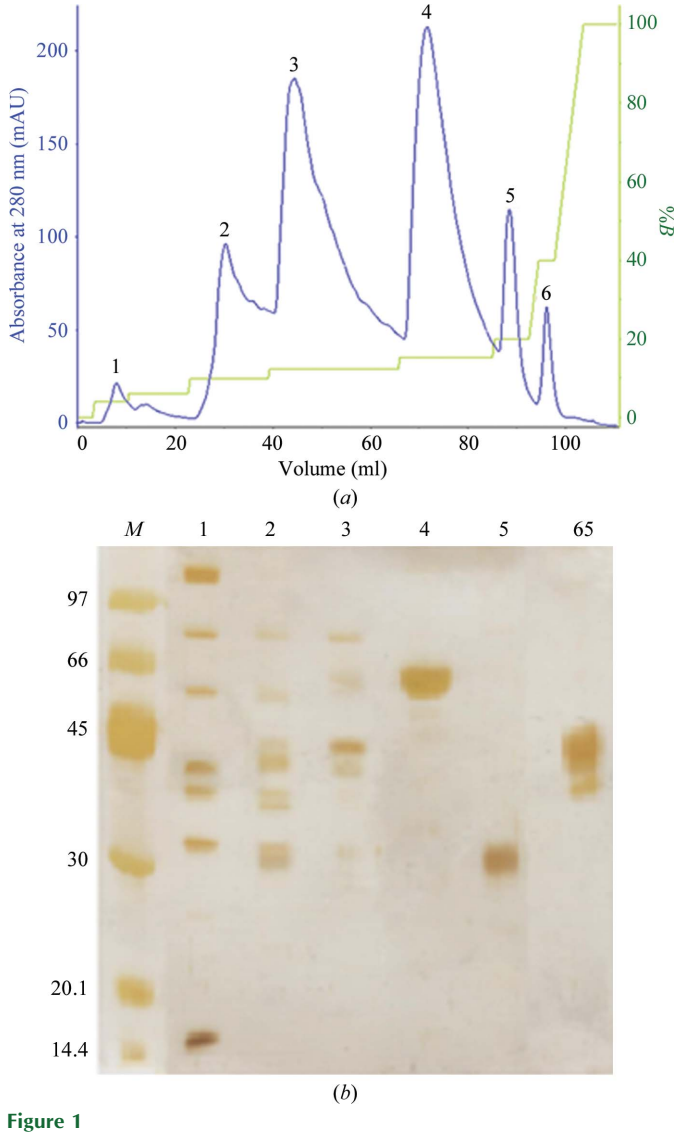

Figure 1
(*a*) Ion-exchange chromatography profile of peak 1 from Sephacryl S-200 size-exclusion chromatography on a Mono S 5/50 GL column. (*b*) SDS–PAGE gel of protein peak fractions from ion-exchange chromatography. Lane *M*, molecular-mass markers (labelled in kDa); lanes 1, 2, 3, 4, 5 and 6 correspond to the chromatographic peak fractions with the same labels. Lane 4 represents LmLAAO.

out using *MOLREP* (Vagin & Teplyakov, 2010) with a model based on the atomic coordinates of native LAAO from *V. ammodytes ammodytes* (PDB entry 3kve; Georgieva *et al.*, 2011).

3. Results and discussion

LmLAAO was purified from the crude venom of *L. muta* by a two-step procedure that involves size-exclusion and ion-exchange chromatography. The size-exclusion chromatography resulted in five peaks which were analyzed by SDS–PAGE (results not shown). The first peak containing LAAO (~60 kDa and yellow in colour) was applied onto a cation-exchange column, which resulted in the further separation of six peaks; the presence of purified LmLAAO (>95%) was confirmed in peak 4 (Figs. 1*a* and 1*b*). The total yield of purified protein was 1.2 mg from 150 mg crude venom. Crystals were obtained when an 11 mg ml^{-1} solution of the purified protein was equilibrated against a reservoir solution consisting of 0.2 *M* ammonium acetate, 20%(*w*/*v*) PEG 3350 pH 7.1 (Fig. 2).

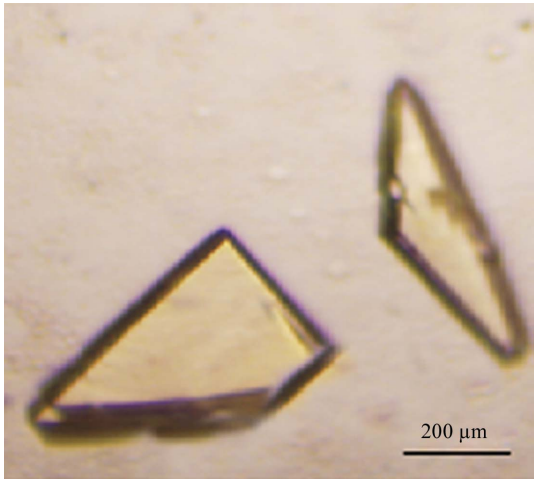

Figure 2
Photomicrograph of the LmLAAO crystals.

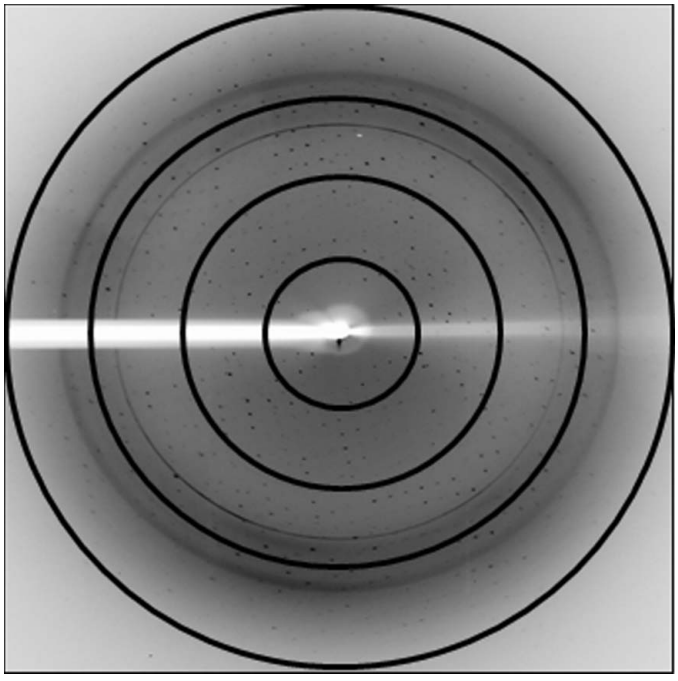

Figure 3
X-ray diffraction pattern. The concentric circles indicate resolutions of 8.0, 5.5, 3.6 and 3.0 Å, respectively.

Table 2
Data collection and processing.

Values in parentheses are for the outer shell.

Diffraction source	Brazilian Synchrotron Light Laboratory
Wavelength (Å)	1.458
Temperature (K)	100
Detector	MAR Mosaic 225 mm
Crystal-to-detector distance (mm)	100
Rotation range per image (°)	1.0
Total rotation range (°)	180
Exposure time per image (s)	90
Space group	$P2_1$
a, *b*, *c* (Å)	66.05, 79.41, 100.52
α, β, γ (°)	90.00, 96.55, 90.00
Mosaicity (°)	1.35
Resolution range (Å)	30.00–3.00 (3.16–3.00)
Total No. of reflections	67669 (9944)
No. of unique reflections	20727 (3016)
Completeness (%)	99.2 (100.0)
Redundancy (multiplicity)	3.3 (3.3)
$\langle I/\sigma(I)\rangle$	5.5 (2.5)
$R_{\rm r.i.m.}$	0.142 (0.379)
Overall *B* factor from Wilson plot (Å^2)	48.0

The LmLAAO crystal diffracted to a maximum resolution of 3.0 Å (Fig. 3) and the reflections were indexed in space group $P2_1$. Taking the molecular weight (~60 kDa) and the presence of two molecules in the asymmetric unit into consideration results in a Matthews coefficient (Matthews, 1968) of 2.18 Å^3 Da^{-1}, which corresponds to a solvent content of 43.7%. Data-collection and processing statistics are presented in Table 2.

The atomic coordinates of the LAAO from *V. ammodytes ammodytes* (PDB entry 3kve; Georgieva *et al.*, 2011), which shares 87% sequence identity with LmLAAO, were used to generate a search model for molecular-replacement calculations carried out using *MOLREP* (Vagin & Teplyakov, 2010). A clear solution was obtained for two molecules in the asymmetric unit in space group $P2_1$. *REFMAC*5 (Murshudov *et al.*, 2011) was used for rigid-body refinement and resulted in an *R* factor of 26.47% and an $R_{\rm free}$ of 34.40%. Structure refinement is currently in progress since the amino-acid sequence of LmLAAO has now been determined (Bregge-Silva *et al.*, 2012)

This research was supported by grants from FAPESP, CNPq, CAPES and DAAD. AU is supported by a FAPESP post-doctoral fellowship.

References

Alves, R. M., Antonucci, G. A., Paiva, H. H., Cintra, A. C. O., Franco, J. J., Mendonça-Franqueiro, E. P., Dorta, D. J., Giglio, J. R., Rosa, J. C., Fuly, A. L., Dias-Baruffi, M., Soares, A. M. & Sampaio, S. V. (2008). *Comp. Biochem. Physiol. A*, **151**, 542–550.
Arima, J., Sasaki, C., Sakaguchi, C., Mizuno, H., Tamura, T., Kashima, A., Kusakabe, H., Sugio, S. & Inagaki, K. (2009). *FEBS J.* **276**, 3894–3903.
Bregge-Silva, C., Nonato, M. C., de Albuquerque, S., Ho, P. L., Junqueira de Azevedo, I. L. M., Diniz, M. R. V., Lomonte, B., Rucavado, A., Díaz, C., Gutiérrez, J. M. & Arantes, E. C. (2012). *Toxicon*, **60**, 1263–1276.
Du, X.-Y. & Clemetson, K. J. (2002). *Toxicon*, **40**, 659–665.
Faust, A., Niefind, K., Hummel, W. & Schomburg, D. (2007). *J. Mol. Biol.* **367**, 234–248.
Fry, B. G. (2005). *Genome Res.* **15**, 403–420.
Georgieva, D., Murakami, M., Perband, M., Arni, R. & Betzel, C. (2011). *Mol. Biosyst.* **7**, 379–384.
Jancarik, J. & Kim, S.-H. (1991). *J. Appl. Cryst.* **24**, 409–411.

Jorge, M. T., Sano-Martins, I. S., Tomy, S. C., Castro, S. C., Ferrari, R. A., Ribeiro, L. A. & Warrell, D. A. (1997). *Toxicon*, **35**, 545–554.
Kang, T. S. *et al.* (2011). *FEBS J.* **278**, 4544–4576.
Kasai, K., Ishikawa, T., Komata, T., Fukuchi, K., Chiba, M., Nozaka, H., Nakamura, T., Sato, T. & Miura, T. (2010). *FEBS J.* **277**, 453–465.
Kitani, Y., Tsukamoto, C., Zhang, G., Nagai, H., Ishida, M., Ishizaki, S., Shimakura, K., Shiomi, K. & Nagashima, Y. (2007). *FEBS J.* **274**, 125–136.
Laemmli, U. K. (1970). *Nature (London)*, **227**, 680–685.
Lewis, R. J. & Garcia, M. L. (2003). *Nature Rev. Drug Discov.* **2**, 790–802.
Li, Z.-Y., Yu, T.-F. & Lian, E. C.-Y. (1994). *Toxicon*, **32**, 1349–1358.
Matthews, B. W. (1968). *J. Mol. Biol.* **33**, 491–497.
Moustafa, I. M., Foster, S., Lyubimov, A. Y. & Vrielink, A. (2006). *J. Mol. Biol.* **364**, 991–1002.
Murshudov, G. N., Skubák, P., Lebedev, A. A., Pannu, N. S., Steiner, R. A., Nicholls, R. A., Winn, M. D., Long, F. & Vagin, A. A. (2011). *Acta Cryst.* D**67**, 355–367.
Nagashima, Y., Tsukamoto, C., Kitani, Y., Ishizaki, S., Nagai, H. & Yanagimoto, T. (2009). *Comp. Biochem. Physiol. B Biochem. Mol. Biol.* **154**, 55–61.
Otwinowski, Z. & Minor, W. (1997). *Methods Enzymol.* **276**, 307–326.
Rodrigues, R. S., da Silva, J. F., França, J. B., Fonseca, F. P., Otaviano, A. R., Silva, F. H., Hamaguchi, A., Magro, A. J., Braz, A. S., dos Santos, J. I., Homsi-Brandeburgo, M. I., Fontes, M. R., Fuly, A. L., Soares, A. M. & Rodrigues, V. M. (2009). *Biochimie*, **91**, 490–501.
Stábeli, R. G., Sant'Ana, C. D., Ribeiro, P. H., Costa, T. R., Ticli, F. K., Pires, M. G., Nomizo, A., Albuquerque, S., Malta-Neto, N. R., Marins, M., Sampaio, S. V. & Soares, A. M. (2007). *Int. J. Biol. Macromol.* **41**, 132–140.
Sun, M.-Z., Guo, C., Tian, Y., Chen, D., Greenaway, F. T. & Liu, S. (2010). *Biochimie*, **92**, 343–349.
Ullah, A., Coronado, M., Murakami, M. T., Betzel, C. & Arni, R. K. (2012). *Acta Cryst.* F**68**, 211–213.
Ullah, A., Souza, T. A., Abrego, J. R., Betzel, C., Murakami, M. T. & Arni, R. K. (2012). *Biochem. Biophys. Res. Commun.* **421**, 124–128.
Vagin, A. & Teplyakov, A. (2010). *Acta Cryst.* D**66**, 22–25.
Yang, H.-H., Yang, S. L., Peng, K.-C., Lo, C.-T. & Liu, S.-Y. (2009). *Mycol. Res.* **113**, 924–932.
Zhang, H., Teng, M., Niu, L., Wang, Y., Wang, Y., Liu, Q., Huang, Q., Hao, Q., Dong, Y. & Liu, P. (2004). *Acta Cryst.* D**60**, 974–977.
Zhang, Y.-J., Wang, J.-H., Lee, W.-H., Wang, Q., Liu, H., Zheng, Y.-T. & Zhang, Y. (2003). *Biochem. Biophys. Res. Commun.* **309**, 598–604.